

Terrestrial volcanic eruptions and their association with solar activity

Irina Vasilieva^{1,+} and Valentina V. Zharkova^{2,3,*+}

¹Main Astronomical Observatory, Golosiivo, Kyiv, Ukraine

²University of Northumbria, Newcastle upon Tyne, UK

³ZVS Research Enterprise Ltd., London, UK

*valentina.zharkova@northumbria.ac.uk

+these authors contributed equally to this work

ABSTRACT

We compare the frequencies of volcanic eruptions in the past 270 years with the variations of solar activity and summary curve of principal components of the solar background magnetic field (SBMF) derived from the WSO synoptic magnetic maps. Quartile distributions of volcanic eruption frequencies over the four phases of a 11 year cycle (growth, maximum, descent and minimum) reveal higher numbers of eruptions occurring at the maxima of SBMF of southern polarity with some increases at the minima of sunspot numbers. The frequency analysis of volcanic eruptions with Morlet wavelet reveals that the period of 22 years is more pronounced than 11 years. Comparison of the volcanic frequencies with the summary curve of SBMF for 11 cycles after 1868 (excluding 1950-1980 affected by the open nuclear bomb testing) reveals a strong correlation with the coefficient of -0.84 (within a confidence interval of 95%), while for 8 cycles in the early period of 1750-1868 the correlation becomes nearly twice lower. This lower correlation was likely to be caused by the geomagnetic jerk and migration of the Earth's magnetic pole to lower latitudes. The maxima of volcanic eruptions are shown to occur during solar activity cycles with the southern magnetic polarity that, in turn, can be associated with stronger disturbances of the geomagnetic field leading to the eruption number increase. The next anticipated maximum of volcanic eruptions is expected to occur during cycle 26 (2031-2042), when the solar background magnetic field will have a southern magnetic polarity. These volcanic eruptions can contribute to terrestrial cooling during the modern grand solar minimum (GSM) (2020-2053).

Introduction

Volcanos occur when the inner energy of Earth under its surface approaches a certain critical level, so that the hot magma, which is under a huge inner pressure, can squirt from the Earth's interior through a weak region of the crust producing volcanos. Geomagnetic storms induced by interplanetary coronal mass ejections, interplanetary magnetic fields and solar wind particles (see, for example¹ and references therein) can cause either sporadic electric currents in the earth locations along the breaks of the surface, which can heat up the surface and reduce their resistivity to the shifts,² or induce the currents leading to piezoelectric tension of the breaks on the surface leading to volcanos.³ Magnetic storms occurring during maximum years of solar activity are found to affect the properties of the faults and gestate in some regions with large earthquakes.^{2,4} A clear correlation was detected between the occurrence of large earthquakes at any terrestrial location and high-speed solar wind streams and/or proton densities, which are known increasing during the maxima of solar activity defined by averaged sunspot numbers.⁵⁻⁸

The Volcanic Explosivity Index (VEI)⁹ was introduced for evaluation of the eruption effects on the terrestrial atmosphere based on the estimation of the volume of volcanic eruption materials (ejected tephra, ashflows, pyroclastic flows etc), the height of the ash column, duration of eruption. The eruptions with the VEI=6 and higher can cause the effect of a volcanic winter - a noticeable cooling of the atmosphere caused by the ash pollution that can, in turn, cause anti-greenhouse effect shielding the solar radiation leading to global cooling. Therefore, volcanic activity can be an important component of the solar-terrestrial interaction.

The early papers tried to link the terrestrial volcanic occurrences with solar activity.¹⁰⁻¹⁶ Later by applying the wavelet analysis to the historical records of large volcanic eruptions other authors managed to establish a connection between the global volcanicity and solar activity cycle of 11 years.^{17,18} Other papers either confirmed^{19,20} or denied²¹ the existence of 11 year cycles in the volcanic eruptions, while some studies showed close relationships between earthquakes, solar activity and volcanic eruptions,^{22,23} though questioned by other researchers.²⁴

This uncertainty exists most likely because there are no viable mechanisms yet proposed for the explanation of any correlation between volcanic activity on the Earth and solar activity. Most of the authors still support the idea that volcanic activity is increased during minima of solar activity^{17,19,21} or during a descending phase of solar activity.²⁵ The increase of

frequency of strong volcanic eruptions during the minima of solar activity was suggested associated with the variation of circulation of atmospheric masses during a solar cycle.²⁶ Their strong variations are suggested to affect the Earth's revolution about its axis that can cause, in turn, moderate earthquakes and volcanos to relieve the tension of the volcanic magma. This mechanism could reduce a probability of powerful volcanic eruptions while increase the number of moderate eruptions.¹⁷

Anderson²⁷ suggested an alternative model, in which the presence of sufficient quantities of volcanic aerosols can change the circulation of the terrestrial atmosphere to such the extent that it would change the velocity of the Earth rotation that, in turn, leading to an increase of earthquakes and eruption of powerful volcanos. While Bumba²⁸ demonstrated possible links of longitudinal distribution of solar magnetic fields with geomagnetic disturbances. Hence, despite definite links between the volcano occurrences and solar activity are not clear yet, the consequences of volcanic eruptions have to be with necessity included in any models of the global climate changes since they may noticeably affect the terrestrial atmosphere.

Although, there was a recent development of finding a new proxy of solar activity, the eigen vectors of the solar background magnetic field (SBMF) derived with the principle component analysis (PCA) from the synoptic magnetic maps captured by the full-disk magnetograph of the Wilcox Solar Observatory, US.^{29,30} The modulus of the summary curve of the two principal components of SBF fits rather closely the averaged sunspot numbers currently used as the solar activity index.^{29,30} The advantage of the new proxy, the summary curve of PCs, is that it not only provides the amplitudes and shapes of solar activity cycles but also captures the leading magnetic polarities in these cycles.

The solar activity was shown to be defined by the solar dynamo action in the two layers of the solar interior producing two magnetic waves having close but not equal periods of about 11 years. The interference of these two magnetic waves leads to a grand period of about 350-400 years for their amplitude oscillations when the normal magnetic wave (and cycle) amplitudes approach grand solar minima (GSM) caused by the wave's beating effect.³⁰ Such the grand periods coincide with well-known GSMs as Maunder minimum (MM), Wolf and Oort and other grand minima.³¹ In fact, the Sun was shown to enter in 2020 the period of a modern GSM lasting until 2053^{30,32} similar to the previous GSM.

During the most recent GSM, MM, the terrestrial temperature was reduced by about 1C,³³ in average, that was associated with the reduction for solar radiation,³⁴ which, in turn, was proxied by the absence of sunspots and active regions on the solar surface during the MM.³¹ Although, the terrestrial temperature was found increasing since Maunder minimum by 0.5C per century,^{35,36} which was first assigned to the increase of solar activity producing a modern warming period.³⁷ However, from cycle 21 the solar activity became systematically decreasing that coincided with a decrease of the solar background magnetic field in the approach of the GSM.^{29,30}

On the other hand, in the past few hundred years the Sun was shown to provide some additional radiation to the Earth by moving closer towards the Earth orbit because of the solar inertial motion (SIM) caused by the gravitation of large planets.^{38,39} These periodic variations of the Sun-Earth distance, and the solar irradiance, occur every 2100-2200 years, called Hallstatt's cycles, which were independently derived from the isotope abundances in the terrestrial biomass.^{40,41} In the current Hallstatt's millennial cycle, the Sun-Earth distances are decreasing from the MM until 2600 that leads to the increase of solar irradiance deposited to the atmosphere of the Earth (and other planets).³⁹ This SIM effect contributes to the terrestrial atmosphere heating, in addition to any heating caused by the greenhouse gasses considered in the terrestrial models.

Hence, there is the interplay between the increase of solar radiation caused by SIM and its reduction caused by the modern GSM in solar activity. These two effects define the resulting temperatures on the Earth with the GSM dominating the next 30 years.^{32,39} Therefore, in this paper we attempt to establish more definite links between the frequency of volcanic activity and the variations of solar activity using both the sunspot numbers⁴² and the new proxy of solar activity linked to the solar magnetic field.³⁰

Observations

Frequency of volcanic eruptions

The information about the volcanic eruptions was derived from the Smithsonian Institution's GVP database including the volcanoes that are known or suspected to have erupted within the Holocene or Pleistocene. The GVP website provides access to the raw data and a history of volcanic eruptions. The main list of Holocene volcanoes contains 1408 volcanoes associated with 9928 eruptions (version 4.10.0 dated May 14, 2021).⁴³ The dates of volcanic eruptions are determined by different methods and with varying precision. There are 2 criteria, which a volcanic eruption must satisfy, in order to be included into this research: it must be accurately dated, and it must be historically confirmed.

Fig. 1 shows the number of eruptions that were observed from 1700 to 2020 (5639 in total, of which 3943 with $VEI \geq 2$). In the last century, the frequency of observed eruptions is higher, and in the twentieth century (1900-1999), 2944 eruptions were observed (of which 1940 with $VEI \geq 2$). However, the fixation of a larger number of the eruptions in recent years is most likely due to changes in the method registrations of the eruptions. According to²⁵ completeness of the dates of volcanic eruptions for $VEI \geq 5$ begins since 1800, for $VEI \geq 4$ - since 1900 and for $VEI \geq 3$ - since 1960. In our analysis, we are assumed that the data gaps are a random process, and the trend in the data has been eliminated by the spline.

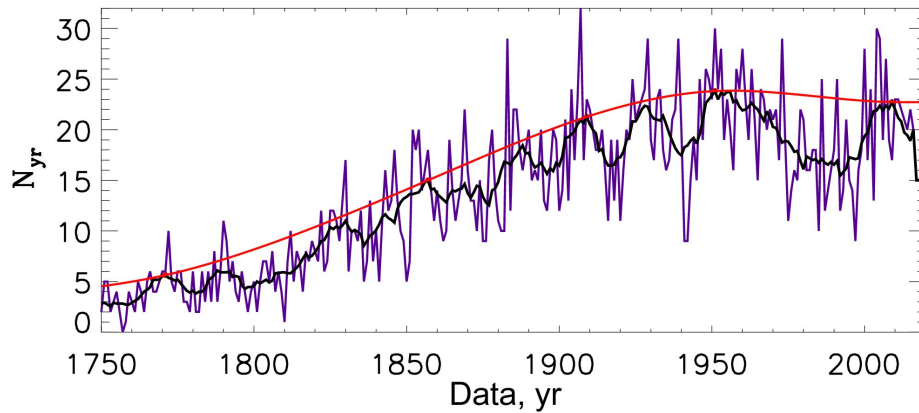


Figure 1. Frequencies of the annual volcanic eruptions in the period of 1700-2020 (violet line). The annual numbers of volcanic eruptions averaged with a running filter of 11 years over-plotted (black line) with the envelope curve marking the maximal magnitudes (red line).

In order to eliminate random variations of the volcanic eruption frequencies, the data was smoothed with the running averaging filter over an 11 year window. By assuming that in the past three centuries the maximal number of volcanic eruptions was similar to that in the past few decades, we have built the envelope curve along the maximal magnitudes of eruption occurrences and carried out the interpolation by spline for the intermediate magnitudes (Fig. 1).

Links with the solar activity phases

Solar activity is currently defined by the average number of sunspots and groups on a solar disk at a given day or month.⁴² There is a well-known 11-year cycle of solar activity,⁴² or a 22-year cycle, during which a complete reversal of the magnetic polarity of the sunspots occurs. The annual numbers of sunspots were taken from the Solar Influences Data Analysis Center (SIDC) at the Royal Observatory of Belgium.⁴⁴

The 25 cycles of solar activity occurred during the period of 270 years from 1750 until 2020 are shown in Fig. 2, top plot. The averaged sunspot numbers are plotted versus the available frequencies of the eruption of volcanos of different significance. It seems that the very strong volcanic eruptions ($VEI \geq 5$) occur during the minima of solar activity defined by the sunspot index.

The distributions of volcanic eruptions in the four quartiles of a solar cycle (yellow line): growth, maxima, descent and minima using the phase dates from⁴⁵ are presented in Table 1 and Fig. 2 (bottom left plot, blue lines) for the whole volcanic dataset excluding only 1950-1990 as likely to be affected by the open nuclear weapon testing). The largest volcanic eruptions are found to occur during the descending and minimal phases of the solar activity defined by sunspots that agrees with the previous findings.^{17,19,21,25}

However, the frequencies of volcanic eruptions calculated for the solar activity cycles provided by the modulus summary curve of the largest eigen vectors of the solar background magnetic field (SBMF)³⁰ shown in Fig. 2, bottom left plot (red lines) demonstrate that the maximal frequencies of volcanic eruptions occur during the maxima of the solar activity defined by the SBFM proxy (see Method section for details). This finding is closer to the other studies of volcanic and earthquake occurrences in the recent century,⁵⁻⁸ showing the maximal frequencies of volcanic eruptions during the maxima of solar activity, or magnetic field.

Some of the discrepancies between the quartile distributions of volcanic eruptions over a solar cycle of 11 years can be caused by the different solar activity indices: sunspots and eigen vectors of SBFM, can be caused by differences between solar activity curves occurred in three cycles in 1730-1760 that is discussed in the forthcoming paper. However, the fact that in the both definitions the number of volcanic eruptions is rather high during the 11 cycle minima, thus, not being affected by the solar activity indices lead us to the conclusion that most likely it is caused by some natural terrestrial phenomena (magnetic jerk and north pole migration) discussed in section below.

Data analysis and discussion

Periods of volcanic activity from the wavelet analysis

By considering time series in the frequency-time space it is possible to derive dominant periods and their variations in time. If the volcanic activity has a periodicity and the dominant one is about 11 years then this would be a good verification of

Table 1. The total number of volcanic eruptions N occurred for a given phase of a solar cycle and % from the total number of eruptions in the cycle derived for several VEI in the period of 1750-2020.

VEI	Growth		Max		Descent		Min		All
	N	%	N	%	N	%	N	%	N
1	171	15.0	269	23.6	324	28.4	375	32.9	1139
2	523	17.0	723	23.5	961	31.3	864	28.1	3071
3	99	16.4	140	23.3	169	28.1	194	32.2	602
4	27	22.4	20	15.9	37	29.4	42	33.3	126
5	5	29.4	3	17.6	2	11.8	7	41.2	17
6	0	0	2	40.0	1	20.0	2	40.0	5
7	0	0	0	0	0	0	1	100.	1
All	825	16.7	1157	23.3	1494	30.1	1485	29.9	4961

the connection between solar and volcanic activity. This point was investigated using a wavelet transform (see the Methods section).¹⁸

The Morlet wavelet analysis was applied to the frequencies of volcanic eruptions reported in section and the result is plotted Fig. 3. The wavelet spectrum of the temporal series of volcanic eruptions in 1750-2020 years reveals the two powerful peaks at 21.4 ± 1.4 years (corresponding to a double 11 year cycle) and at 55.6 ± 10.5 years (its nature is unknown yet). While the peak near the period of 10.7 ± 0.9 (close to the duration of a single solar activity cycle) is much less pronounced. This double cycle feature motivates us to investigate the link for volcanic eruptions with the solar activity proxy of SBMF variations, which, unlike the sunspot index, contain also the magnetic polarity for each cycle.

Volcanic eruption frequency and solar background magnetic field

Let us compare the temporal variations of the frequency of volcanic eruptions and variations of the summary curve of the PCs, or the eigen vectors, of the SBMF³⁰ defining the solar activity during the solar cycles from 1750 to 2020. In order to compare the frequencies of volcanic eruptions with variations of the summary curve of the PCs of SBMF, the arbitrary amplitudes of the summary curve variations were normalised by its maximal magnitude. The comparison of these two series with the frequencies of volcanic eruptions inverted from minima on the top to maxima at the bottom is shown in Fig. 4.

It the period 1868 - 1950 and 1990-2020 the frequency of volcanic eruptions reveals a clear pattern of its maxima following the maxima or the descending phase of the magnetic field curve with the southern polarity while minima fit rather close the maxima or ascending phase of the magnetic field maxima with the northern polarity. While in the earlier years (1762-1868) and in the years of 1950-1980 this link disappeared. Hence, the volcanic eruption frequencies are found following the solar magnetic field variations with a smaller degree of correlation for 8 cycles before 1868 and with much higher correlations for 11 cycles in 1868- 1950 and 1990-2020.

The correlation of this normalised summary curve with volcanic eruption frequencies presented in Fig. 4 gave the correlation coefficient of -0.21 for the whole set of data. Since there were two sections 1762-1868 and 1868-1950 where the series show different properties, then we also looked at the correlation of the series "by parts". The correlation coefficient was 0.46 with a 95% confidence interval of [0.4124, 0.5051] for the period of volcanic eruptions in 1762-1868, while reaching the magnitude of -0.84 with a 95% confidence interval of [-0.8574, -0.8207] for the volcanic eruptions in the period of 1868-1950. The disappearance of a link with the solar or terrestrial magnetic fields in 1950s to 1980 s can be linked to the open nuclear bomb testing as the link is restored a few decades after after this testing was banned.

Hence, the volcanic eruption frequencies have maxima every 22 years during the periods when the summary curves have the southern polarity. This coincides with the period of 22 years found from the volcanic frequencies in the wavelet section using the Morlet wavelet. Also the total numbers of volcanic eruptions shown in Fig. 2 (bottom right plot) during a 22 year cycle (red line) for the period of 1750-1868 (black curve) and 1868-1950 (indigo curve) confirm that the maximum eruptions of occurs during the maxima of solar activity cycles of SBMF with southern magnetic polarity. This finding is in line with the other studies showing the high speed solar wind streams or energetic proton fluxes to be the drivers of the most powerful earthquakes.⁶⁻⁸

Furthermore, a strong correlation of the frequencies of volcanic eruptions in 1868-1950 and solar cycles with the southern magnetic polarity can be understood in the terms of accepted views that the increase of geomagnetic disturbances often correspond to an increase in the interplanetary magnetic field of the southern polarity (see, for example,^{5,46-50}). A possible reason for the lower correlation in thee early years of 1750-1868 is suggested in section below.

Volcanic eruptions and the motion of the North pole

The Carrington solar event in 1859, the largest recorded solar magnetic event, has been associated with the external field changes with the minimum -1760 nT at the Colaba magnetic Observatory in Bombay.^{51,52} Also, there is the evidence that a geomagnetic jerk has occurred around 1860.^{53,54} The geomagnetic jerk is a relatively abrupt change in the rate of secular variations in one or more parameters of the Earth's magnetic field. One of the most powerful geomagnetic jerks was observed during of 1969-1970. Until about 1971, the northern magnetic pole moved more or less uniformly at a speed of about 10 km/year, then suddenly began to accelerate. This acceleration of the pole motion is associated with the so-called geomagnetic jerk that occurred in 1969-1970.^{53,54}

The geomagnetic jerk, which took place around 1860, may help to explain the change in direction of the northern magnetic pole, which was suggested when considering earthquakes.⁵⁵ Another possible confirmation of the internal restructuring of the Earth in the 60s of the 19th century may be a sharp change in the direction of the motion of the Earth's magnetic pole (Fig. 5) according to model calculations.⁵⁶

In 1760-1860, the magnetic pole was moving away (see Fig. 5), and after 1861 it began returning back by rapidly approaching the geographic pole of the Earth. This position was approached as close as possible in 2018, and the magnetic pole began to move away again. These dates coincide very well with the periods identified by us from a comparison of the number of volcanic eruptions and the SBMF variations.

Conclusions

In this paper we explored the frequencies of volcanic eruptions in the past two centuries and their possible links to the variations of solar activity and solar background magnetic field. Contrary to,¹⁷ we obtained a dominant 22-year period of volcanic activity (VEI ≥ 2 , 3829 eruptions) and a much weaker peak for a period of 10.7 years. More volcanic eruptions are found to occur during maximum phases of the doubled solar cycles of 22 years of SBMF when the solar background magnetic field has a southern polarity.

We established a high correlation of the number of volcanic eruptions with the solar background magnetic field during the period of 1868-1950 and much lower correlation during the period 1750-1868. The strong correlation recorded in 8 cycles of SBMF after 1868 suggests that possible physical mechanisms of volcanic eruptions are linked to the increased solar activity features, e.g. the solar background (poloidal) magnetic field, energetic particles of solar wind and solar flares and large-scale shocks produced by interacting solar magnetic loops of the toroidal field.

This link of volcanic eruptions with the solar background magnetic field is likely to include electro-magnetic interaction of the SBMF with the terrestrial magnetic field causing geomagnetic disturbances^{5,46-49} that can lead to shifts of the crusts, most powerful earthquakes⁶ and volcanic eruptions. This can be also influenced by the perturbations of energetic particles and waves on the Earth's air masses¹⁷ or an increase in precipitation¹⁷ that can lead to an increase in the tectonic /volcanic instability.

The possible reasons of a reduced correlation between volcanic eruptions and solar activity index recorded in the period of 1750-1868 can be associated with the geomagnetic jerk and related migration of the North pole towards lower latitudes. Although, some of the differences between the distributions of eruption frequencies over the solar cycles of 11 years can be related to the differences in solar activity indices defined by sunspots and eigen vectors of magnetic fields related to different types of solar magnetic fields: toroidal and poloidal, that is discussed in the forthcoming paper. While the lack of correlation in 1950-1980 can be linked to the open air nuclear bomb testings that distorted the effects of the solar magnetic field.

In summary, the increase of volcanic eruptions established during the solar cycles with the southern polarity of SBMF emphasises the importance of solar-terrestrial interaction in volcanic eruptions. This link can also play an important role in the next few decades affected by the modern Grand Solar Minimum (2020-2053)^{30,32} because in cycle 26 the solar magnetic field will have the southern polarity. This can lead to a potential increase of volcanic eruptions and additional terrestrial cooling during the modern GSM.^{17,19,21}

Methods

Wavelet transform

Wavelet transform of signals is the development of spectral analysis methods. Unlike Fourier analysis, the wavelet transform gives a two-dimensional scan of the analysed signal, while the time coordinate and frequency are independent variables. This representation allows you to explore the properties signal simultaneously in time and frequency spaces. Wavelet analysis is excellent a tool for examining signals with time-varying frequency characteristics.

The choice of the mother wavelet is dictated by the task and the nature of the signal under study. When we use the Morlet wavelet (the real part of it is damped function of cosine), we obtain a high frequency resolution, which is important for our task.

Solar background magnetic field as a new solar activity proxy

Principle Component Analysis was applied to the low-resolution full disk solar background magnetic field (associated with the poloidal magnetic field) measured by the Wilcox Solar Observatory to derive the dominant eigenvalues covering the maximum variance of the data³⁰ corresponding to the eigenvectors, or Principal Components (PCs), which came as a pair.

These PCs are considered to be a reflection of the main (dipole) dynamo waves in the solar poloidal magnetic field produced by the dynamo mechanism.³⁰ The PCs were classified by applying the symbolic regression approach based on the Hamiltonian principle⁵⁷ and deriving the mathematical formulae describing the amplitude and phase variations.²⁹

This summary curve of these two PCs derived for cycles 21-23 and predicted for cycle 24-26 is plotted in Fig. 6 (top plot) also showing the variations of the dominant solar background magnetic field: northern for positive and southern for negative amplitudes. The prediction of the summary curve to cycles 25 and 26 presented in Fig. 6 (top plot) taken from Fig. 2, bottom plot in³⁰) shows a noticeable decrease of the predicted average sunspot numbers in cycle 25 to $\approx 80\%$ of that in cycle 24 and in cycle 26 to $\approx 40\%$ that is linked to a reduction of the amplitudes and an increase of phases of the principal components of SBMF. The prediction of the summary curve by thousand years backward and forward presented in Fig.3³⁰ revealed the occurrence of grand solar cycle of 350-400 years, reproducing the well-known Maunder, Wolf, Oort, Homeric and many other Grand Solar Minima.

This summary curve was proposed³⁰ as a new solar activity proxy since the module of the summary curve fits rather closely the averaged sunspot numbers currently used as a solar activity index (Fig. 6, bottom plot). A remarkable resemblance between the modulus summary curve and the curves describing the averaged smoothed sunspot numbers or the averaged sunspot magnetic flux in cycles 21-23 with some small exception for the descending phase of cycle 23, which was later explained by the strongly inflated sunspot numbers used at Locarno observatory.⁵⁸ After their correction, the averaged sunspot numbers in cycle 23 fit rather closely the modulus summary curve presented in Fig. 6.

Hence, from the one hand, this modulus summary curve is found to be a good proxy of the traditional solar activity contained in the averaged sunspot numbers. On the other hand, this summary curve is a derivative from the principal components of SBMF with clear mathematical functionalities representing at the same time the real physical process - poloidal field dynamo waves - generated by the solar dynamo.³⁰

The suggestion of usage of the summary curve of two eigen vectors, or principle components of the solar background magnetic field as a new proxy of solar activity has been recently supported by other predictions of the solar activity in cycle 25^{59,60} obtained from the same solar magnetic field components measured from the same WSO magnetic synoptic maps as those reported earlier.^{29,30}

Acknowledgments

The authors wish to express their deepest gratitude to the respected reviewers of the paper for their constructive comments, from which the paper strongly benefited. In addition, the authors would like to thank the Smithsonian Institution staff for providing the access to the GVP database containing the volcanic eruption data and the Solar Influences Data Analysis Center (SIDC) at the Royal Observatory of Belgium for providing the averaged sunspot numbers. The authors also express their deepest gratitude to the staff and directorate of Wilcox Solar Observatory, Stanford, US, for providing the coherent long-term observations of full disk synoptic maps of the solar background magnetic field.

Author contributions statement

I.V. gathered and processed the volcanic frequency data while V.Z. provided and analysed the solar background magnetic field data. V.Z. and I.V. compared and analysed the results, wrote and reviewed the manuscript.

Additional information

The authors do not have any competing financial interests.

References

1. Stamper, R., Lockwood, M., Wild, M. N. & Clark, T. D. G. Solar causes of the long-term increase in geomagnetic activity. *J. Geophys. Research* **104**, 28325–28342 (1999).
2. Han, Y., Guo, J. & Ma, C. Possible triggering of solar activity to big earthquakes (Ms8) in faults with near west-east strike in China. *Sci. China Ser. B: Phys. Mech. Astron* **47**, 173–181 (2004).
3. Sobolev, N. V. & Demin, V. M. *Mechano-electrical Phenomena in the Earth*, 215pp (Nauka, 1980).

4. Love, J. J. & Thomas, J. N. Insignificant solar-terrestrial triggering of earthquakes. *Geophys. Res. Letters* **40**, 1165–1170 (2013).
5. Gonzalez, W. D., Tsurutani, B. T. & Clúa de Gonzalez, A. L. Interplanetary origin of geomagnetic storms. *Space Sci. Reviews* **88**, 529–562 (1999).
6. Odintsov, S., Boyarchuk, K., Georgieva, K. & Atanasov, D. Long-period trends in global seismic and geomagnetic activity and their relation to solar activity. *J. Physics and Chemistry of the Earth* **31**, 88–93 (2006).
7. Martichelli, V., Harabaglia, P., Troise, C. & De Natale, G. On the correlation between solar activity and large earthquakes worldwide. *Scientific Reports* **10**, 11495 (2020).
8. Martichelli, V., Harabaglia, P., Troise, C. & De Natale, G. On the Long Range Clustering of Global Seismicity and its Correlation With Solar Activity: A New Perspective for Earthquake Forecasting. *Front. Earth Sci* **10**, , doi = doi:10.3389/feart.2020.595209 (2020).
9. Newhall, C. & Self, S. The Volcanic Explosivity Index (VEI): An Estimate of Explosive Magnitude for Historical Volcanism. *J. Geophys. Research* **87**, 1231–1238 (1982).
10. Kluge, E. *Ueber Synchronismus und Antagonismus von vulkanischen Eruptionen und die Beziehungen derselben zu den Sonnenflecken und erdmagnetischen Variationen* (Engelmann, Leipzig, 1863).
11. De Marchi, L. Nuove Teorie Sulle Cause Dell 'Era Glaciale'. *Scientia* **5**, 310 (1911).
12. Köppen, W. Parallelismus zwischen der häufigkeit der sonnenflecken und der vulkanausbrüche. *Himmel und Erde* **8**, 529–532 (1896).
13. Lyons, C. J. Sun Spots and Hawaiian Eruptions. *Monthly Weather Review* **27**, 144 (1899).
14. O'Reilly, J. P. On the dates of volcanic eruptions and their concordance with the sun-spot period. *Proceedings of the Royal Irish Academy (1889-1901)* **5**, 392–432 (1898). URL <http://www.jstor.org/stable/20490557>.
15. Jensen, H. I. Possible relation between sunspot minima and volcanic eruptions. *Journal and Proceedings of the Royal Society of New South Wales* **36**, 42–60 (1902).
16. Sapper, K. Cycles of volcanic activity. *Volcano Letters* **302**, 2–4 (1930).
17. Stothers, R. B. Volcanic eruptions and solar activity. *J. Geophys. Research* **94**, 17371–17381 (1989).
18. Mazzarella, A. & Palumbo, A. Does the solar cycle modulate seismic and volcanic activity. *J. Volcanology and Geothermal Research* **39**, 89–93 (1989).
19. Casati, M. Significant statistically relationship between the great volcanic eruptions and the count of sunspots from 1610 to the present. In *EGU General Assembly Conference Abstracts*, EGU General Assembly Conference Abstracts, 1385 (2014).
20. Ma, L., Yin, Z. & Han, Y. Possible influence of solar activity on global volcanicity. *Earth Science Research* **7**, 110 (2018).
21. Střeštitk, J. Possible correlation between solar and volcanic activity in a long-term scale. In Wilson, A. (ed.) *Solar Variability as an Input to the Earth's Environment*, vol. 535 of *ESA Special Publication*, 393–396 (2003).
22. Schneider, S. H. & Mass, C. Volcanic Dust, Sunspots, and Temperature Trends. *Science* **190**, 741–746 (1975).
23. Kelly, A. C. The evolving Earth Observing System (EOS) mission operations concept: then and now. In *ESA Special Publication*, vol. 1 of *ESA Special Publication*, 106–113 (1996).
24. Lockwood, M. & Owens, M. J. Implications of the Recent Low Solar Minimum for the Solar Wind during the Maunder Minimum. *Astrophys. J. Letters* **781**, L7 (2014).
25. Herdiwijaya, D., Johan, A. & Nurzaman, M. Z. On the Relation between Solar and Global Volcanic Activities. In *Proceedings of the 2014 International Conference on Physics*, 105–108 (Atlantis Press, 2014/10). URL <https://doi.org/10.2991/icp-14.2014.21>.
26. Gray, L. J. *et al.* Solar influences on climate. *Reviews of Geophysics* **48** (2010). URL <https://agupubs.onlinelibrary.wiley.com/doi/abs/10.1029/2009RG000282>.
27. Anderson, D. L. Earthquakes and the Rotation of the Earth. *Science* **186**, 49–50 (1974).
28. Bumba, V. Solar local magnetic fields and their relations to the background fields. *Contributions of the Astronomical Observatory Skalnaté Pleso* **15**, 495 (1986).
29. Shepherd, S. J., Zharkov, S. I. & Zharkova, V. V. Prediction of Solar Activity from Solar Background Magnetic Field Variations in Cycles 21-23. *Astrophysical J.* **795**, 46 (2014).

30. Zharkova, V. V., Shepherd, S. J., Popova, E. & Zharkov, S. I. Heartbeat of the Sun from Principal Component Analysis and prediction of solar activity on a millenium timescale. *Scientific Reports* **5**, 15689 (2015).
31. Eddy, J. A. The Maunder Minimum. *Science* **192**, 1189–1202 (1976).
32. Zharkova, V. Modern grand solar minimum will lead to terrestrial cooling. *Temperature* **7**, 217–222 (2020a). URL <https://doi.org/10.1080/23328940.2020.1796243>.
33. Easterbrook, D. J. *Evidence-based Climate Science* (Elsevier, 2016).
34. Lean, J., Beer, J. & Bradley, R. Reconstruction of solar irradiance since 1610: Implications for climate change. *Geophys. Res. Letters* **22**, 3195–3198 (1995).
35. Parker, D. E., Jones, P. D., Folland, C. K. & Bevan, A. Interdecadal changes of surface temperature since the late nineteenth century. *J. Geophys. Research: Atmospheres* **99**, 14373–14399 (1994). URL <https://agupubs.onlinelibrary.wiley.com/doi/abs/10.1029/94JD00548>.
36. Akasofu, S.-I. On the recovery from the little ice age. *Natural Science* **2**, 1211–1224 (2010).
37. Lockwood, M., Stamper, R. & Wild, M. N. A doubling of the Sun’s coronal magnetic field during the past 100 years. *Nature* **399**, 437–439 (1999).
38. Zharkova, V. V., Shepherd, S. J., Zharkov, S. I. & Popova, E. RETRACTED ARTICLE: Oscillations of the baseline of solar magnetic field and solar irradiance on a millennial timescale. *Scientific Reports* **9**, 9197 (2019).
39. Zharkova, V. Millennial Oscillations of Solar Irradiance and Magnetic Field in 600-2600. *chapter in a book "Solar system planets and exoplanets"* 30 pp. (2021).
40. Steinhilber, F., Beer, J. & Fröhlich, C. Total solar irradiance during the Holocene. *Geophys. Res. Letters* **36**, L19704 (2009).
41. Steinhilber, F. *et al.* 9,400 years of cosmic radiation and solar activity from ice cores and tree rings. *Proceedings of the National Academy of Science* **109**, 5967–5971 (2012).
42. Wolf, R. Studies on the frequency of Sun-spots, and on their connexion with the Magnetic Declination-variation. *Monthly Notices of Royal Astron.Soc.* **30**, 157 (1870).
43. Global Volcanism Program, G. Volcanoes of the World, v. 4.10.0 (14 May 2021) (2013). URL <https://doi.org/10.5479/si.GVP.VOTW4-2013>. Downloaded June 9, 2021.
44. SILSO World Data Center. The International Sunspot Number. *International Sunspot Number Monthly Bulletin and online catalogue* (2021).
45. Vasilyeva, I. Is there any connection between solar activity and earthquakes? *Space Science and Technology (Ukraine)* **26**, 90–102 (2020).
46. Maezawa, K. Dependence of the magnetopause position on the southward interplanetary magnetic field. *Planetary and Space Science J.* **22**, 1443–1453 (1974).
47. Perreault, P. & Akasofu, S. I. A study of geomagnetic storms. *Geophys. Journal* **54**, 547–573 (1978).
48. Stauning, P. Coupling of IMF B_Y variations into the polar ionospheres through interplanetary field-aligned currents. *J. Geophys. Research* **99**, 17309–17322 (1994).
49. Stauning, P., Clauer, C. R., Rosenberg, T. J., Friis-Christensen, E. & Sitar, R. Observations of solar-wind-driven progression of interplanetary magnetic field B_Y -related dayside ionospheric disturbances. *J. Geophys. Research* **100**, 7567–7586 (1995).
50. Prosovetsky, D. & Myagkova, I. The correlation between geomagnetic disturbances and topology of quasi-open structures in the solar magnetic field. *Geomagnetism and Aeronomy* **51** (2011).
51. Cliver, E. W. & Dietrich, W. F. The 1859 space weather event revisited: limits of extreme activity. *Journal of Space Weather and Space Climate* **3**, A31 (2013).
52. Manda, M. & Chambodut, A. Geomagnetic field processes and their implications for space weather. *Surveys in Geophysics* **41** (2020).
53. Newitt, L., Manda, M., McKee, L. & Orgeval, J.-J. Recent acceleration of the north magnetic pole linked to magnetic jerks. *EOS Transactions* **83**, 381 (2002).
54. Newitt, L. & Dawson, E. Secular variation in north america during historical times. *Geophys. J. of the Royal Astronomical Society* **78**, 277–289 (2007).

55. USGS, U.S. Geological Survey. Earthquake Hazards Program (2021). URL <https://earthquake.usgs.gov/earthquakes/search/>. Accessed June 7, 2019.
56. NGDC, The National Geophysical Data Center. Wandering of the Geomagnetic poles (2021). URL <https://www.ngdc.noaa.gov/geomag/GeomagneticPoles.shtml>. Accessed July 23, 2021.
57. Schmidt, M. & Lipson, H. Distilling free-form natural laws from experimental data. *Science* **324**, 81–85 (2009).
58. Clette, F., Svalgaard, L., Vaquero, J. M. & Cliver, E. W. Revisiting the Sunspot Number. A 400-Year Perspective on the Solar Cycle. *Space Science Reviews* **186**, 35–103 (2014).
59. Kitiashvili, I. N. Application of Synoptic Magnetograms to Global Solar Activity Forecast. *Astrophysical J.* **890**, 36 (2020). [1910.00820](https://arxiv.org/abs/1910.00820).
60. Obridko, V. N., Sokoloff, D. D., Pipin, V. V., Shibalvaa, A. S. & Livshits, I. M. Zonal harmonics of solar magnetic field for solar cycle forecast. *arXiv e-prints* arXiv:2108.10527 (2021). [2108.10527](https://arxiv.org/abs/2108.10527).

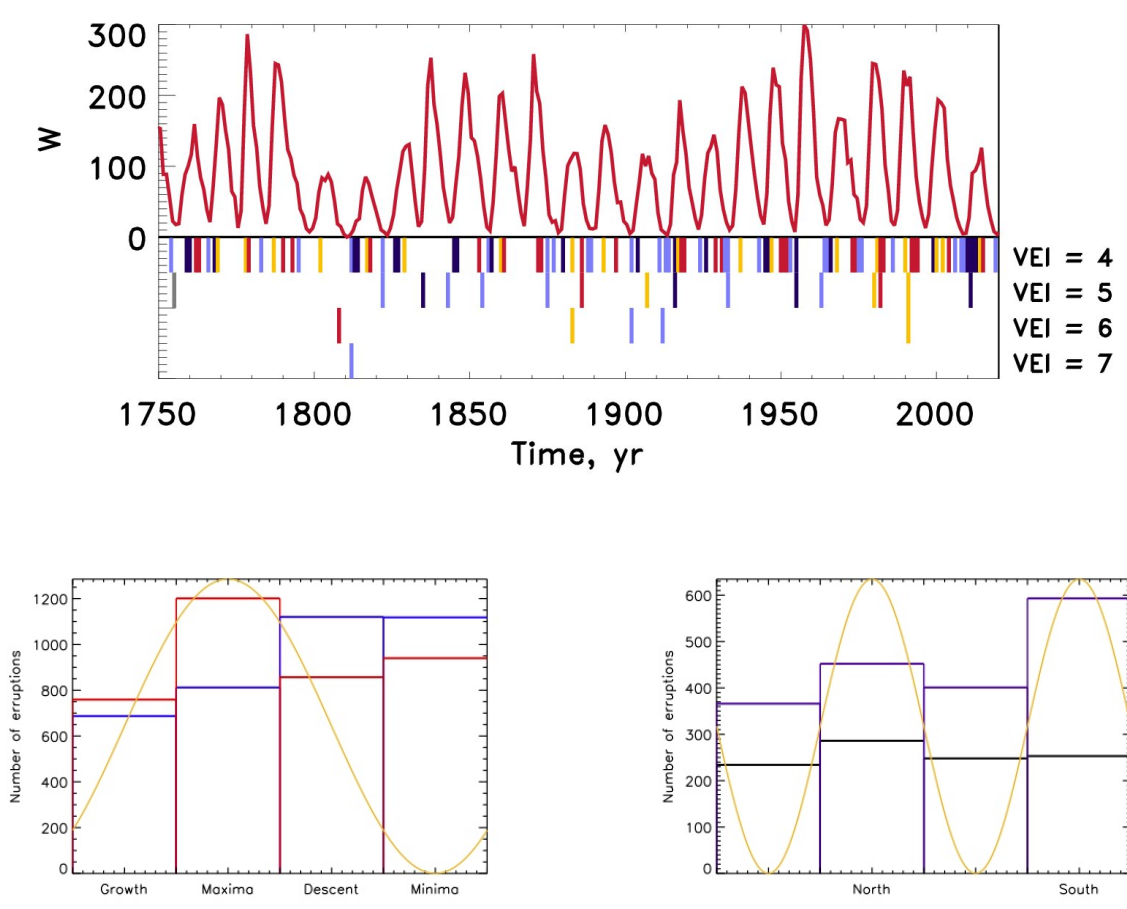


Figure 2. Top: the Wolf numbers describing solar activity and bottom: the dates of eruption volcanos of different significance. The colours define the phases of solar activity cycles: blue - ascending, yellow - maxima, red descending and light blue - minima. Bottom left: a summary of the top plot (and Table 1) showing the volcanic eruption numbers (blue lines) (Y-axis) occurring during the four quartiles of an 11 year solar cycle (yellow line) (X-axis): growth, maximum, descending and minimum phases defined by sunspots (blue lines) and solar background magnetic field (SBMF) (red lines). Bottom right: the volcanic eruption numbers (Y-axis) occurring during a 22 year solar cycle (yellow line) (X-axis) with northern and southern magnetic polarities defined by SBF for the periods of 1750-1868 (black line) and of 1868-1950 & 1990-2020 (indigo line).

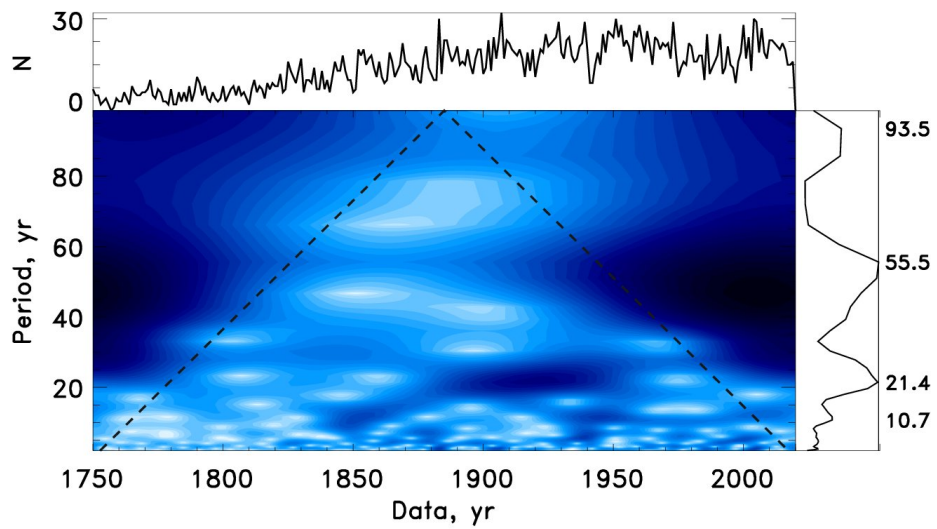


Figure 3. Time series of the annual volcanic eruptions in the period of 1750-2020 (top). The wavelet power spectrum, using the Morlet wavelet. The x-axis is the wavelet location in time. The y-axis is the wavelet period in years. The cone of influence given by the dashed line. The global wavelet spectrum and the main periods of volcanic eruptions (right).

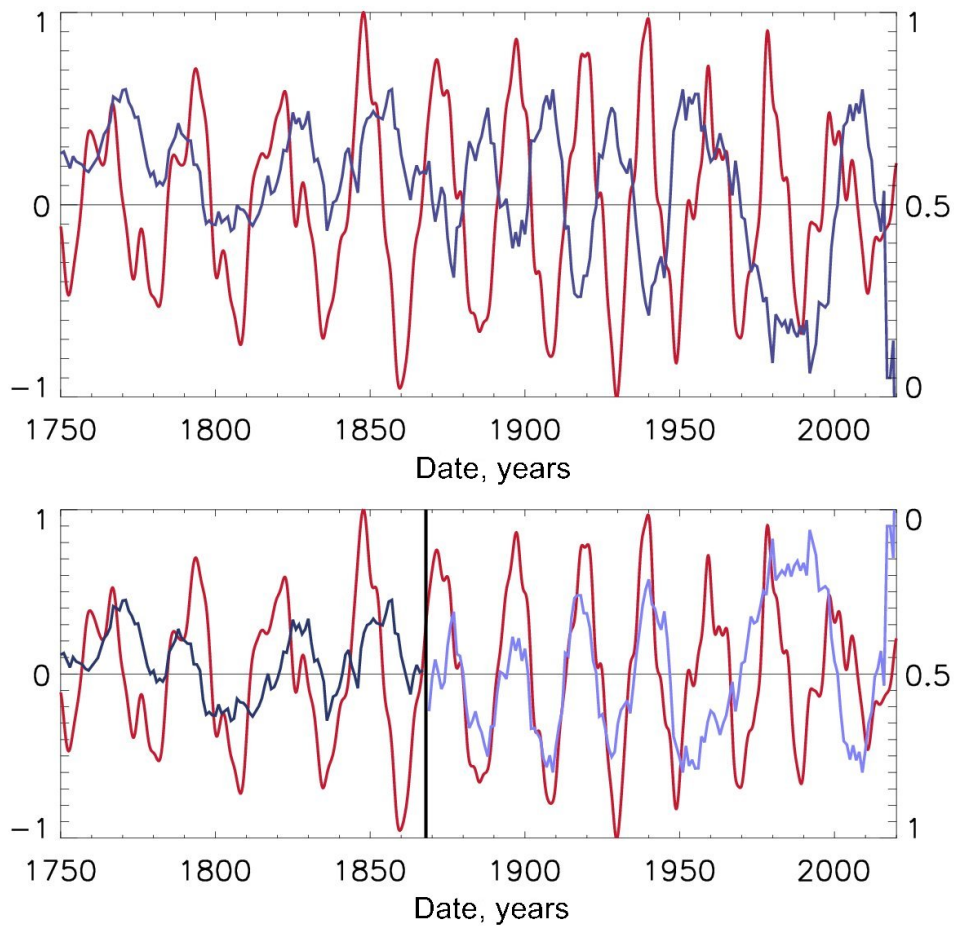


Figure 4. Top plot: The summary curve of solar background magnetic field³⁰ (red curve) normalised by maximum (the left Y-axis) versus the averaged normalised number of volcanic eruptions (blue curve) (the right Y-axis). Positive magnitudes of summary curve correspond to the northern polarity while negative to the southern polarity. Bottom plot: the summary (red) curve versus the volcanic eruption numbers (blue curve) plotted in the inverted scale (from minimum on the top to maximum at the bottom) (the right Y-axis). See the text for the correlation coefficients between these two curves and their confidence intervals.

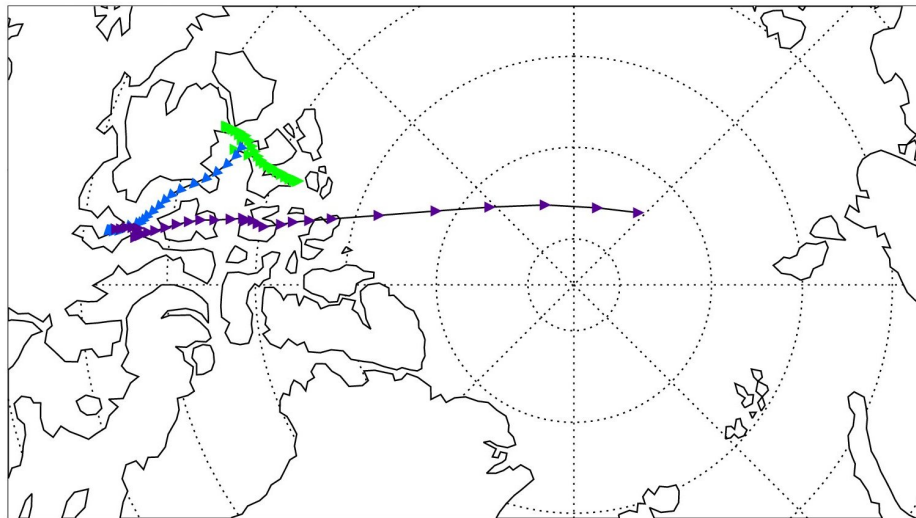


Figure 5. Reconstructed locations of the north magnetic pole from 1500 to 2020.⁵⁶

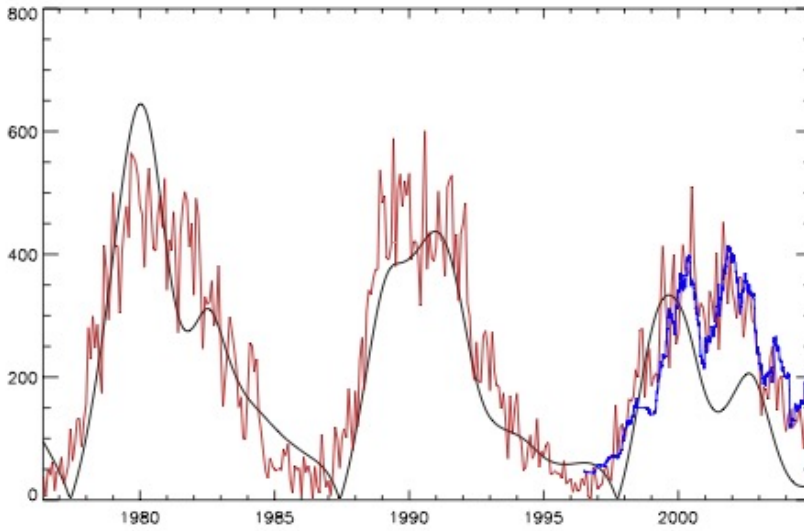
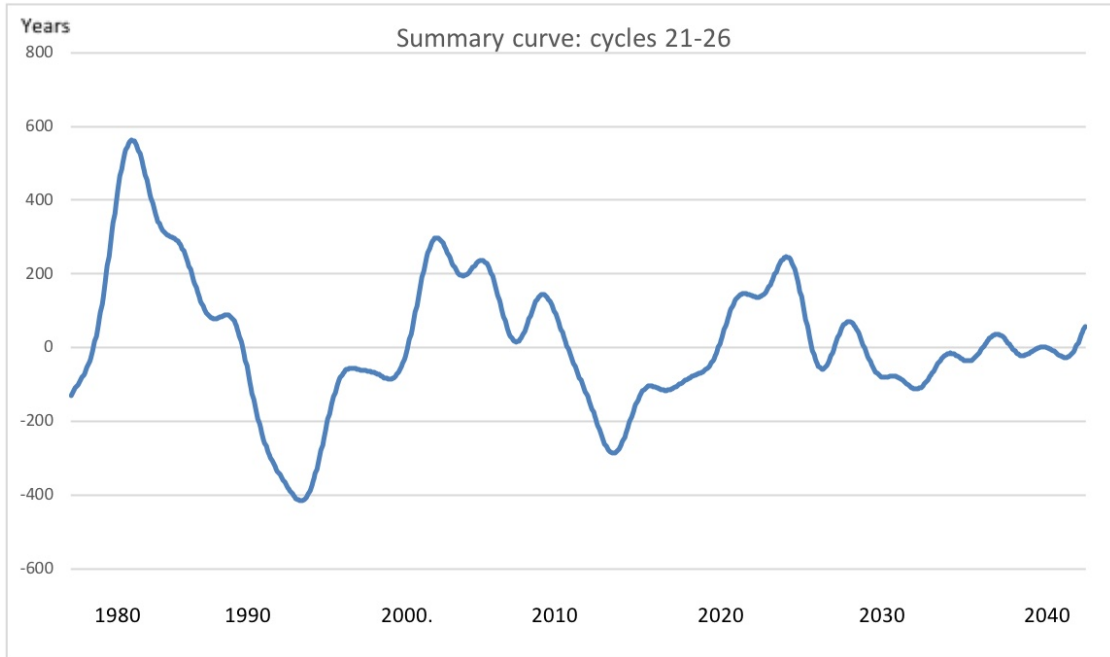


Figure 6. Top plot: The summary curve derived from the data for cycles 21-23 and extrapolated to cycles 24, 25 and 26 (taken from^{30,32}). Bottom plot: Modulus summary curve, derived from the summary curve above for cycles 21-23 overplotted on the averaged sunspot numbers used as the current solar activity index (taken from³⁰).